On Segmental Mobility in a Compatible Poly(α-methylstyrene)-*block*-polystyrene Copolymer

Sean Curran*

Analytical Sciences Laboratory, Allied-Signal Inc., Morristown, New Jersey 07960

Jin Kon Kim and Chang Dae Han*

Department of Chemical Engineering, Polytechnic University, Brooklyn, New York 11201

Received December 26, 1991; Revised Manuscript Received April 7, 1992

ABSTRACT: The segmental mobility in a compatible poly(α-methylstyrene)-*block*-polystyrene (PαMS-*block*-PS) copolymer was investigated, using solid-state nuclear magnetic resonance (NMR) spectroscopy. For the study, a series of PαMS-*block*-PS copolymers containing various amounts of PαMS (from 13 to 81 wt %) were synthesized via anionic polymerization. The results of differential scanning calorimetry (DSC) showed a very broad, single glass transition temperature (T_g) for all block copolymers studied. However, measurements of the spin–lattice relaxation rate in the rotating frame ($T_{1\rho H}$) via cross polarization in NMR as a function of temperature indicate that the block copolymer has microheterogeneity at temperatures above the onset point of the glass transition but becomes homogeneous as the temperature approaches the midpoint of the glass transition. NMR spectroscopy indicates further that there is a distribution of segmental mobilities, with the PS and PαMS strongly influencing each other.

Introduction

Measurement of the glass transition temperature (T_g) has long been used for investigating the miscibility of polymer blends,[1] as well as for determining whether or not microphase separation has taken place in block copolymers.[2-8] Using dynamic mechanical measurements, Robeson et al.[2] determined T_gs of binary blends of poly(α-methylstyrene) (PαMS) and polystyrene (PS) and poly(α-methylstyrene)-*block*-polystyrene (PαMS-*block*-PS) copolymers. On the basis of the detection of a single value of the loss tangent in dynamic mechanical measurements, Robeson et al. concluded that PαMS-*block*-PS copolymers had no microdomains (i.e., homogeneous) when the molecular weight of each block was less than about 150 000. Using differential scanning calorimetry (DSC) to measure T_g, Dunn and Krause[3] investigated macrophase (liquid–liquid) separation in binary blends of PαMS and PS and microphase separation in PαMS-*block*-PS copolymers. Subsequently, others[9-12] also investigated, via DSC, the phase behavior of binary blends of PαMS and PS.

What appears to be in common for both binary blends and diblock copolymers of PαMS and PS is that the glass transition takes place over a very broad range of temperatures, especially for samples containing an almost equal proportion of the constituent components. Phalip et al.[8] showed that plots of T_g, based on the midpoint of the transition, of PαMS-*block*-PS copolymers versus composition have negative deviations from linearity, following the Fox equation, similar to that often observed for compatible blend systems.

Recently we synthesized, via anionic polymerization, a series of PαMS-*block*-PS copolymers having widely varying block length ratios. Using DSC we measured the T_gs of the block copolymers and found that they exhibited very broad, single glass transition temperatures. It should be mentioned that DSC cannot detect the segmental mobility of polymer molecules with dimensions less than ca. 100 nm.

However, solid-state nuclear magnetic resonance (NMR) spectroscopy offers an ideal tool for the investigation of microheterogeneity in polymer blends or block copolymers. There are two parameters which are accessible by NMR analysis: chemical shift and relaxation rates. If the constituent components have unique chemical shifts, one can monitor the responses of the individual components. In particular, the proton relaxation behavior of the constituent components can be measured independently. Since spin diffusion rapidly equilibrates ^1H relaxation rates within a given domain, variations in the spin–lattice relaxation rate (T_{1H}) or the spin–lattice relaxation rate in the rotating frame ($T_{1\rho H}$) can be used to measure heterogeneity on the nanometer scale.[13-21]

The classic NMR method for investigation of the miscibility of polymer blends on a molecular level is $T_{1\rho H}$ analysis. If two components are intimately mixed on a molecular level, both components display the same $T_{1\rho H}$ because of rapid spin diffusion. In the past such analyses have been applied to a number of polymer blends.[13-24] Obviously such analyses require sufficiently different $T_{1\rho H}$ to differentiate the pure components.

Spin diffusion is a process analogous to thermal diffusion where the temperature gradients between domains are in fact "spin temperature" gradients. A highly polarized spin has a spin temperature close to absolute zero. As the spin temperature increases, the spins approach equilibrium polarization.

If we have isolated domains, they will have different spin temperatures since they have different relaxation rates and therefore approach equilibrium spin temperature at distinct rates characteristic of the given domain. The spin temperature within a given domain reequilibrates very rapidly via homonuclear ^1H dipolar coupling, but some time will pass before the spin temperature can equilibrate across domain boundaries and diffuse to the center of the domains. The time required for this process is controlled by the rate of spin diffusion and the size of the domains. Such rates have been measured, and therefore the time dependence of the rate of equilibration can be used to determine the domain size.[16]

In the present study we applied the same concept to investigate whether or not there might be microheterogeneity in the PαMS-*block*-PS copolymers that had been used for DSC measurements, as mentioned above. Measurements of NMR relaxations as a function of temperature provided information on microheterogeneity throughout the temperature range where DSC exhibits a single

0024-9297/92/2225-4200$03.00/0

Table I
Summary of the Molecular Characteristics of the PαMS-*block*-PS Copolymers and Corresponding Homopolymers Synthesized

	PαMS block or homopolymer		PαMS-*block*-PS copolymer		(wt %)	
sample code	M_w (×10⁻³)	M_w/M_n	M_w (×10⁻³)	M_w/M_n	GPC	NMR
CVI	21	1.07	21–167	1.09	11	13
CIV	50	1.08	50–130	1.08	29	28
CI	54	1.06	54–94	1.08	40	41
BII	52	1.06	52–70	1.08	45	47
CII	99	1.07	99–145	1.09	46	48
CIII	135	1.07	135–120	1.09	59	57
CV	122	1.06	122–26	1.06	83	81
PS-200	195	1.07			0	
PαMS-50	67	1.06			100	
PαMS-75	80	1.07			100	
PαMS-100	98	1.07			100	

T_g. Fortunately, PαMS and PS each has a unique chemical shift which enabled us to independently measure spin relaxation rates. We will show below, based on solid-state NMR spectroscopy, that the PαMS-*block*-PS copolymer which is apparently compatible, as evidenced by a single glass transition temperature and optical clarity, is in fact heterogeneous on a molecular level at temperatures where the glass transition occurs.

Experimental Section

Materials. A series of PαMS-*block*-PS copolymers were synthesized via anionic polymerization, the details of which are described in a previous paper of Kim and Han.[25] A summary of the molecular weights and molecular weight distributions determined for the block copolymers as well as for the corresponding homopolymers is given in Table I. It can be seen in Table I that both homopolymers and block copolymers synthesized in this study can be regarded as nearly monodisperse. We employed, also, NMR spectroscopy (Varian T-60) to determine the weight fraction of the PαMS block in PαMS-*block*-PS copolymer. For the measurements all samples were dissolved in $CDCl_3$ (10 wt % solid) using 1,4-dioxane as the standard material. Using calibration curves the weight fraction of PαMS in a PαMS-*block*-PS copolymer was determined, the results of which for the seven block copolymers synthesized for this study are given in the last column of Table I, indicating that two different experimental techniques, GPC and NMR, give rise to essentially the same weight fraction of PαMS in each block copolymer sample.

Differential Scanning Calorimetry. The T_g for each of the PαMS-*block*-PS copolymers synthesized was measured using a Perkin-Elmer DSC 7 Series unit. Prior to measurement, the base line was obtained using two empty aluminum pans, which was later used for base-line correction. The DSC samples were prepared by compression molding at room temperature. Conditions used for typical DSC runs were to first heat the sample to 230 °C at a rate of 10 °C/min and then anneal it for 2 min and subsequently to quench the sample to 35 °C at a rate of 200 °C/min. During each run nitrogen gas was directed into the DSC cell in order to minimize degradation of the sample. This cycle was repeated several times. Reproducibility of the value of T_g was found to be accurate to within ±1.5 °C.

Solid-State Nuclear Magnetic Resonance Spectroscopy. All solid-state ^{13}C NMR spectra were acquired on a Chemagnetics CMX-300 NMR spectrometer, operating at 300 MHz for ^1H and 75 MHz for ^{13}C. ^1H 90° pulses were 5 μs. $T_{1\rho H}$ relaxation rates were measured via cross polarization using a 500-μs contact time, 50-kHz spin lock, and 75-kHz decoupling after a variable-time (0.1–30 ms) spin lock on ^1H. Temperatures were controlled to within ±0.1 °C. The magic angle was set within 0.1° using the sidebands in the ^{79}Br spectrum of KBr[26] prior to spectrum acquisition. The samples were spun at the magic angle at 4–5 kHz.

Results and Discussion

Glass Transition Behavior of PαMS-*block*-PS Copolymers. Figure 1 gives traces of DSC thermograms

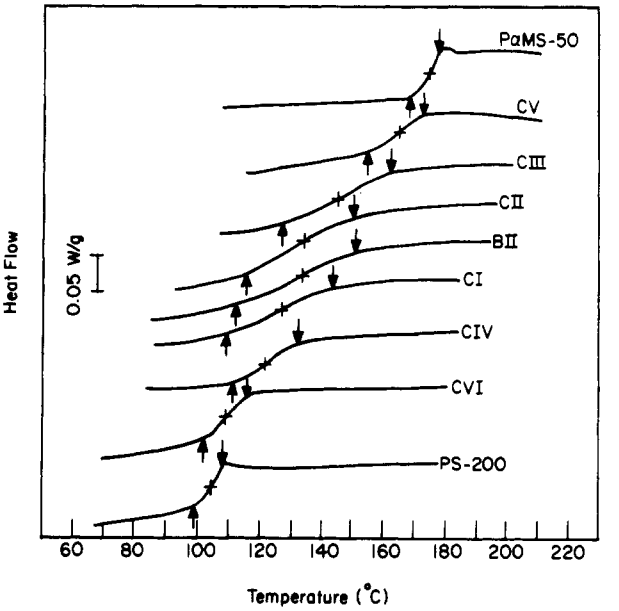

Figure 1. Traces of the DSC thermograms for the homopolymers, PS and PαMS, and seven PαMS-*block*-PS copolymers synthesized in this study (see Table I for the block molecular weights of each sample). The heating rate employed was 10 °C/min. On each curve, the arrow pointing upward on the left side denotes the temperature (T_{gi}) at which the transition begins and the arrow pointing downward on the right side denotes the temperature (T_{gf}) at which the transition ends.

Table II
Summary of the Glass Transition Temperatures for the PαMS-*block*-PS Copolymers Synthesized

sample code	onset point T_{gi} (°C)	midpoint T_{gm} (°C)	final point T_{gf} (°C)
PS-200	100	104	109
CVI	103	109	115
CIV	111	122	132
CI	110	127	145
BII	113	134	152
CII	115	135	152
CIII	128	145	163
CV	154	164	173
PαMS-50	170	175	179

for the homopolymers PS and PαMS and PαMS-*block*-PS copolymers synthesized for this study. It can be seen in Figure 1 that each block copolymer sample has a single value of T_g and that the value of T_g of the block copolymer increases monotonically as the weight fraction of the PαMS diblock increases. In reference to Figure 1, the range of the transition is indicated by two arrows, one pointing upward on the left side to indicate the onset of the transition (T_{gi}) and the other pointing downward on the right side to indicate the final point of the transition (T_{gf}). Table II gives a summary of T_{gi}, T_{gf}, and the midpoint (T_{gm}) of the transition for the seven PαMS-*block*-PS copolymers and constituent homopolymers synthesized for this study, showing that samples BII and CII having almost equal lengths of PαMS and PS block have the largest values of $\Delta T = T_{gf} - T_{gi}$. Earlier, other research groups[3,4] also reported similar observations for PαMS-*block*-PS copolymers, as well as for PαMS-*block*-PS-*block*-PαMS and PS-*block*-PαMS-*block*-PS copolymers.

The dependence of the T_g of PαMS-*block*-PS copolymers on block composition determined in this study is summarized in Figure 2, in which the dotted circles represent the midpoint (T_{gm}) of the transition, the dotted triangles represent the initial point (T_{gi}) of the transition, and the dotted squares represent the final point (T_{gf}) of the transition. In order to facilitate our discussion, we

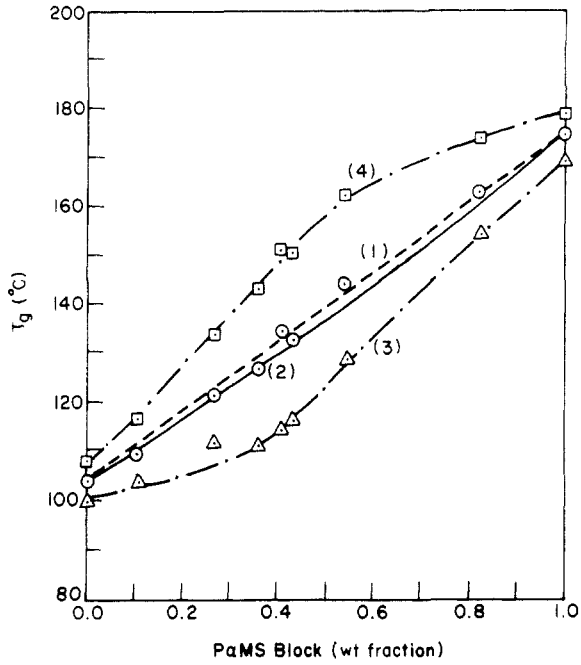

Figure 2. Plots of glass transition temperature (T_g) versus weight fraction of PαMS in the PαMS-*block*-PS copolymers synthesized in this study, in which ⊙ represent the midpoint, ▲ represent the initial point (T_{gi}), and ◻ represent the final point (T_{gf}) in the transition. Here curve 1 describes the prediction based on a linear relationship, curve 2 describes the prediction based on Fox's equation, curve 3 is drawn through the data points of T_{gi}, and curve 4 is drawn through the data points of T_{gf}.

have drawn four curves in Figure 2, namely, curve 1 representing the prediction with the linear relationship $T_g = w_{P\alpha MS}T_{g,P\alpha MS} + w_{PS}T_{g,PS}$ and curve 2 representing the prediction with the Fox equation[27]

$$1/T_g = w_{P\alpha MS}/T_{g,P\alpha MS} + w_{PS}/T_{g,PS} \quad (1)$$

Curve 3 is drawn through the data points representing T_{gi}, and curve 4 is drawn through the data points representing T_{gf}. Note in eq 1 that $w_{P\alpha MS}$ and w_{PS} are the weight fractions of the PαMS and PS blocks, respectively, in the block copolymer and $T_{g,P\alpha MS}$ and $T_{g,PS}$ are the glass transition temperatures of the PαMS and PS blocks, respectively. In plotting curves 1 and 2 given in Figure 2, we used $T_{g,P\alpha MS}$ = 175 °C and $T_{g,PS}$ = 104 °C, as determined in this study. It can be seen in Figure 2 that the measured values of T_{gm} (dotted circles) are in good agreement with the prediction by eq 1. We also observe in Figure 2 that the linear relationship works equally well. It should be mentioned that, very recently, Suzuki and Miyamoto[28] made a theoretical prediction that the T_g of compatible block copolymers would follow the linear relationship. Such a prediction appears to have validity if we choose the midpoint of the transition as the T_g of the PαMS-*block*-PS copolymers investigated in the present study. It is worth pointing out, however, that in Figure 2 we observe *negative* deviations from linearity when using T_{gi} and *positive* deviations from linearity when using T_{gf}. This then puts us in a dilemma as to which of the three curves in Figure 2 represents the true dependence of T_g on block copolymer composition.

It should be pointed out that the smallest size that can be detected by DSC is about 100 nm, which is not sufficiently small enough to probe segmental mobility in a PαMS-*block*-PS copolymer. We speculate here that the PαMS and PS segments in a PαMS-*block*-PS copolymer can move around with their own mobilities and not with the average mobility of the block copolymer.

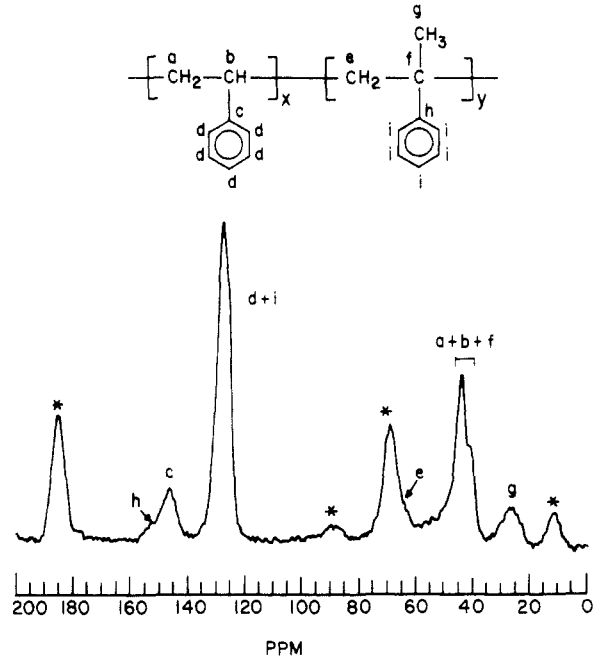

Figure 3. CP-MAS spectrum of sample CII. The peak assignments are noted on the figure, where asterisks denote spinning sidebands generated by MAS at rates lower than the width of the chemical shift anisotropy.

Segmental Mobility in a PαMS-*block*-PS Copolymer As Determined by Solid-State NMR Spectroscopy. It is well established that $T_{1\rho H}$ can be a sensitive measure of the extent of miscibility of two components on a molecular level.[13-21] However, there is insufficient resolution in a solid-state ^1H spectrum to measure this directly for each component. On the other hand, there is sufficient resolution in a ^{13}C spectrum to resolve the components, but ^{13}C relaxation rates reflect individual environments rather than domain structure. Cross polarization (CP), which involves polarization transfer from ^1H to ^{13}C provides a signal where the chemical shift of the ^{13}C allows us to monitor individual components, while the intensity reflects ^1H relaxation.

The spectrum in Figure 3 shows the response, which is essentially a sum of the spectra for the individual blocks of the PαMS-*block*-PS copolymer, for the block copolymer sample CII containing 48 wt % PαMS. The methyl group of PαMS is well resolved from any PS resonance, which makes it ideal for the $T_{1\rho H}$ analysis. The peak at 40 ppm is a mixture of the methylene and methine of PS and the quaternary aliphatic carbon of PαMS. We know that the cross-polarization rate (T_{IS}^{-1}) for the quaternary aliphatic is significantly lower than that for protonated carbons (T_{IS} = 30 μs versus 1.1 ms for protonated versus unprotonated). Thus we use a relatively short contact time, 500 μs, which is insufficient to generate significant polarization for the PαMS carbon. A 500-μs contact time generates a strong response from the protonated (PS backbone) carbons without a significant nonprotonated carbon signal. Shorter contact times give poor signal-to-noise ratios while longer contact times generate a response from the quaternary aliphatic carbon of PαMS.

The intensity in a CP spectrum depends on T_{IS} and $T_{1\rho H}$. The signals grow at different rates, and this variation introduces a complication in variable CP contact time measurements. This is why we chose to use a variable spin lock on the ^1H which monitors $T_{1\rho H}$ at a fixed contact time which eliminates the problems associated with T_{IS}.[13] Thus the peak intensities in a given spectrum are not necessarily quantitative, but their dependence on spin lock times can still be measured.

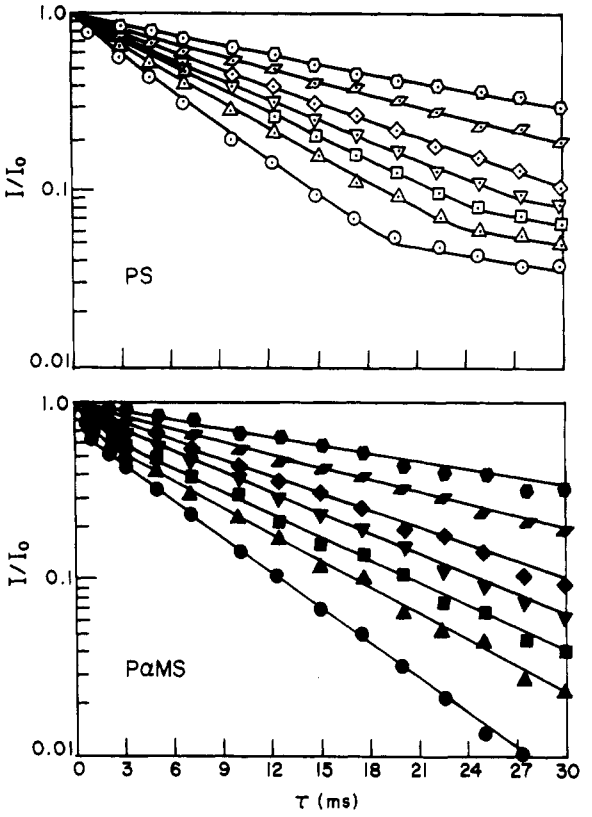

Figure 4. Plots of normalized intensity (I/I_0) versus ^{1}H spin lock hold time (τ) for sample CII at various temperatures (°C): (⊙,●) 30; (▲,▲) 60; (⊡,■) 90; (▼,▼) 120; (◇,◆) 160; (▰,▰) 190; (◎,●) 220.

In addition to $T_{1\rho H}$ measurements to monitor changes in domain structure, we can use variations of the carbon spin–lattice relaxation time (T_{1C}) to characterize high-frequency motions of the individual carbons. As the polymers become more mobile, T_{1C} decreases. Thus we can use a relatively short cycle time in Bloch decay (BD) experiments to determine what fraction of the sample is mobile at any given temperature. Thus we can use the combination of $T_{1\rho H}$ and T_{1C} to characterize homogeneity in a PαMS-*block*-PS copolymer and to see how the two blocks affect each other's molecular mobility.

The $T_{1\rho H}$ relaxation curves, plots of normalized intensity (I/I_0) versus ^{1}H spin lock hold time (τ), for sample CII are given in Figure 4, where I is the intensity for a given hold time and I_0 is the theoretical intensity for zero hold time. Note that, although the intensities are not directly quantitative, we can determine the decay rates from Figure 4. Since the signal decays via spin–lattice relaxation in the rotating frame ($T_{1\rho H}$), the slopes of the curves are determined by $T_{1\rho H}^{-1}$. Both PS and PαMS blocks in sample CII show multiple relaxation rates at temperatures between 30 and 120 °C but a single relaxation curve at temperatures above 120 °C. It should be remembered that the onset of the glass transition for sample CII begins at 115 °C (see Table II). Notice in Figure 4 that the major portion of the relaxation curves at temperatures below 160 °C gives identical relaxation rates for both PαMS and PS blocks, indicating that spin diffusion has equilibrated relaxation rates. Thus, we can conclude that at lower temperatures a major portion of the blocks is well mixed on a molecular level. At temperatures above 160 °C both PS and PαMS give equivalent, single relaxations rates. This indicates the disappearance of microheterogeneity and the formation of a single, homogeneous phase.

The portion where the relaxation rates deviate from this single major relaxation rate indicates isolated domains where spin diffusion has not yet equilibrated relaxation rates. In reference to Figure 4, the slopes of the curves in these areas are consistent with PS- and PαMS-rich domains. These domains are not extremely large; given typical spin diffusion rates,[16] the times required for spin diffusion are consistent with sizes on the order of 5–10 nm. It is known that rapid rotation of the methyl group will reduce spin diffusion rates. Even if that is the case, the only effect will be to change the domain size estimates somewhat, but the conclusions will be unaffected. In addition, since exactly the same effects are observed for the PS backbone where there is no such problem, the conclusions will still stand: these block copolymers are microheterogeneous at temperatures below the midpoint of the T_g.

As discussed above, BD spectra with short cycle times allow us to monitor how the molecular mobility for the individual components depends on temperature. By using spin counting we can quantitatively measure what fraction of each component becomes mobile. The intensity in a ^{13}C BD experiment depends on T_{1C}. If one waits $5T_{1C}$, then the intensities will be directly quantitative. On the other hand, if one does not allow sufficient time between pulses, longer relaxing species will be suppressed. Typical T_{1C}s for highly mobile polymers are relatively short (100 ms to 2 s), while T_{1C}s for typical glassy polymers are relatively long.

In the present study, we measured BD spectra with 10-s cycle times which is sufficient to allow observation of highly mobile carbons while suppressing rigid carbons. Thus we can measure the total intensity (count spins) and determine how much of the sample has become mobile at a given temperature. Since we do not use the same amount of material in each sample, we cannot use intensities to directly compare the level of mobile carbons in each sample. However, by comparing intensities at a given temperature to the intensity in the melt, where all the carbons are mobile, one can determine what fraction of the material has become mobile at that temperature. In Figure 5 are given ^{13}C NMR intensities (normalized by comparison with the total intensity in the melt) in a BD experiment as a function of temperature, i.e., plots of the mobile fraction of a PS block (dotted circle) or a PαMS block (dotted triangle) in sample CII versus temperature. Also given in Figure 5 are, for comparison purposes, ^{13}C NMR intensities for homopolymer PS (closed circle) and homopolymer PαMS (closed triangle). The results given in Figure 5 describe how the two components (i.e., PαMS and PS blocks) affect each other's segmental mobility in sample CII. It can be seen in Figure 5 that the PS block has significantly reduced its mobility (compare dotted circles with closed circles), while the PαMS block has increased its mobility (compare dotted triangles with closed triangles) at all temperatures below 220 °C.

The combined $T_{1\rho H}$ and BD results indicate that sample CII is in fact heterogeneous at the onset point (115 °C) of the glass transition and becomes homogeneous as the temperature approaches the final point (152 °C) of the transition (see Table II). It can be seen in Figure 5 that the segmental mobility of a PαMS block in the PS-rich domains is greater than that of pure PαMS, while the segmental mobility of a PS block in the PαMS-rich domains is restricted, as compared to that of pure PS. The entire sample does not become mobile (rubbery) until well above the glass transition temperature observed via DSC.

The NMR results for the block copolymer sample CIV containing 28 wt % PαMS are given in Figures 6 and 7, and the NMR results for the block copolymer sample CV

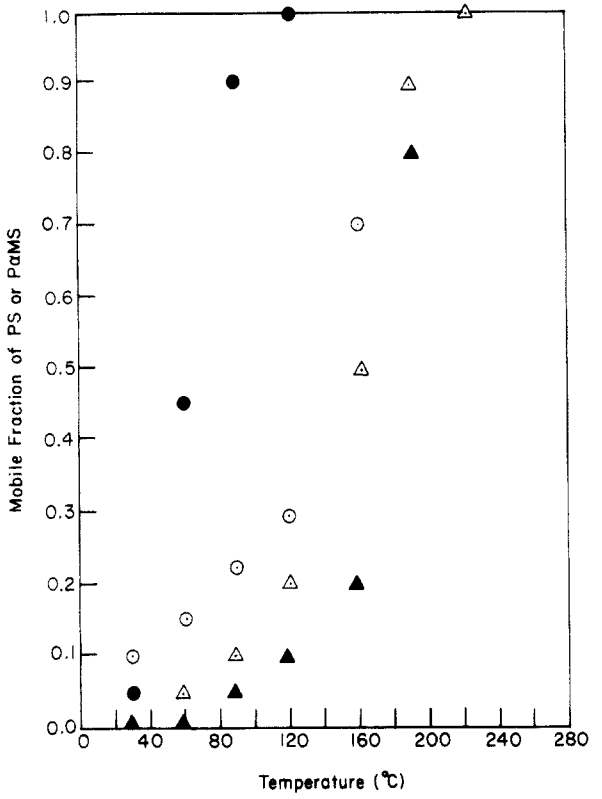

Figure 5. Plots of the mobile fraction of a PS block (⊙) or a PαMS block (▲) in sample CII versus temperature, in which ^{13}C NMR intensities for homopolymer PS (●) and homopolymer PαMS (▲) are also given.

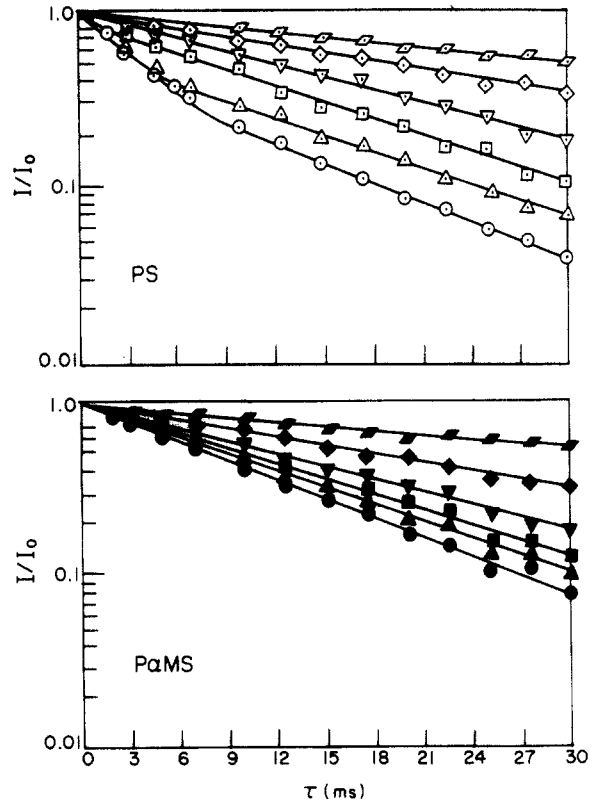

Figure 6. Plots of normalized intensity (I/I_0) versus ^1H spin lock hold time (τ) for sample CIV at various temperatures (°C): (⊙,●) 30; (▲,▲) 60; (⊡,■) 90; (▼,▼) 120; (◇,◆) 160; (▰,▰) 140.

containing 81 wt % PαMS are given in Figures 8 and 9. Again, we observe heterogeneity in the $T_{1\rho H}$ relaxations of PS, and the BD results show restrictions to the segmental mobility of a PS block by a PαMS block and the increased segmental mobility of a PαMS block in the presence of a

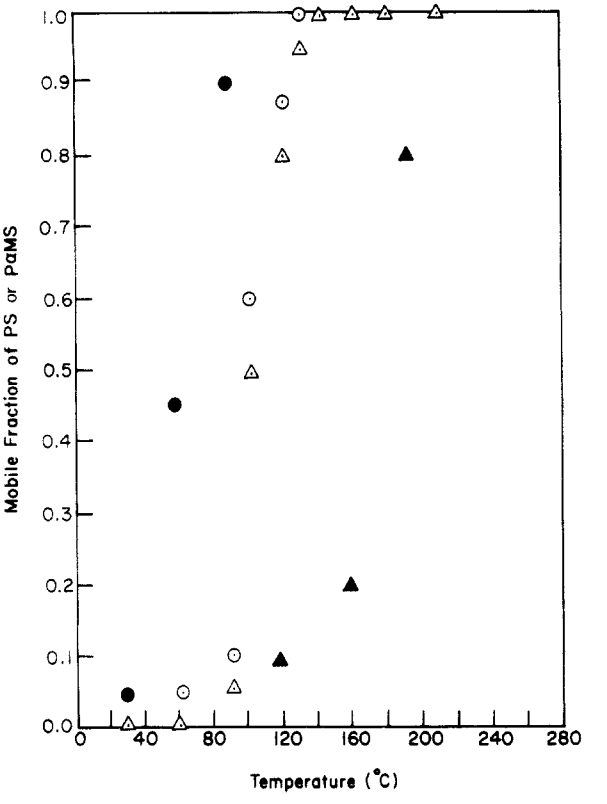

Figure 7. Plots of the mobile fraction of a PS block (⊙) or a PαMS block (▲) in sample CIV versus temperature, in which ^{13}C NMR intensities for homopolymer PS (●) and homopolymer PαMS (▲) are also given.

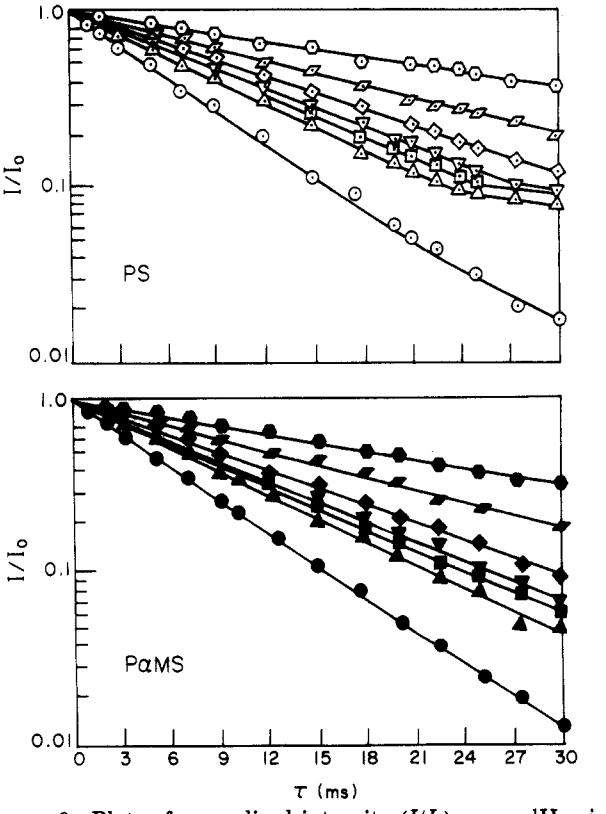

Figure 8. Plots of normalized intensity (I/I_0) versus ^1H spin lock hold time (τ) for sample CV at various temperatures (°C): (⊙,●) 30; (▲,▲) 60; (⊡,■) 90; (▼,▼) 120; (◇,◆) 160; (▰,▰) 190; (◎,●) 220.

PS block. It can be seen, however, in Figures 6 and 8 that, in both samples CIV and CV, the $T_{1\rho H}$ curves for PS show multiple relaxations. The break in the $T_{1\rho H}$ curves for PS (see Figures 4, 6, and 8) occurs because we are dealing

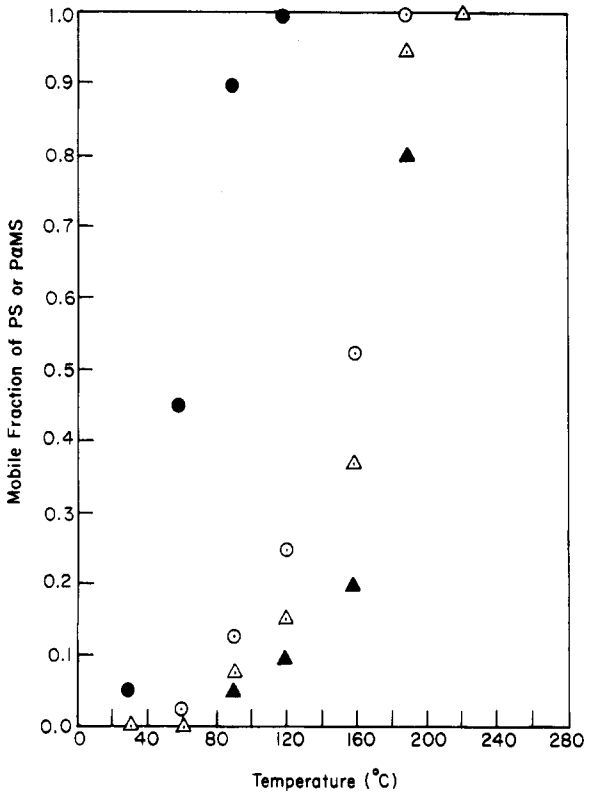

Figure 9. Plots of the mobile fraction of a PS block (⊙) or a PαMS block (▲) in sample CV versus temperature, in which ^{13}C NMR intensities for homopolymer PS (●) and homopolymer pαMS (▲) are also given.

with microheterogeneity. The curve is a sum of the individual relaxations, and the exact time of the break point depends on block copolymer composition and spin diffusion rates. Thus, a PS-rich sample such as CIV will have a relaxation curve dominated by the PS-rich regions, and the break in the curve occurs quite early. The $T_{1\rho H}$ curves for PαMS indicate the presence of only one component. In the case of sample CIV, this is reasonable since the PαMS is such a small fraction (28 wt %) of the total block copolymer that one might expect the probability of PαMS-rich domains to be quite small, while the PS will necessarily have some PS-rich domains.

One might then expect exactly the opposite type of behavior in the block copolymer sample CV where PαMS is the predominant component (81 wt %), but this is not observed. Rather we again observe in Figure 8 multiple relaxations for PS and a single relaxation for PαMS. At present we cannot explain why this is the case, but the intensity variations in the early part of the relaxation curve may simply be dominated by the large signal from the homogeneously mixed regions.

Concluding Remarks

We have shown in this paper that when a PαMS-*block*-PS copolymer has a very broad glass transition temperature as determined by DSC, solid-state NMR spectroscopy can be used to determine whether or not microheterogeneity can be present in the block copolymer at temperatures where the glass transition actually takes place. Solid-state NMR spectroscopy can also be used to determine the presence of microheterogeneity in binary blends of homopolymers. It is worth noting, however, that Roland and co-workers[29-31] observed no microheterogeneity via solid-state NMR spectroscopy in binary mixtures of polyisoprene and poly(vinylethylene) while the blends show very broad, single glass transition temperatures. Their observations appear to suggest to us that the existence of a broad single glass transition temperature in a binary blend does not necessarily indicate the presence of microheterogeneity. Whether this will be the case for other polymer blends is not known at present, because there is no sufficient experimental evidence to generalize. In a future paper, using solid-state NMR spectroscopy we will compare the difference(s), if any, in segmental mobility between PαMS-*block*-PS copolymer and binary blends of PαMS and PS.

References and Notes

(1) Olabisi, O.; Robeson, L. M.; Shaw, M. T. *Polymer–Polymer Miscibility*; Academic Press: New York, 1979; Chapter 3.
(2) Robeson, L. M.; Matzner, M.; Fetters, L. J.; McGrath, J. E. In *Recent Advances in Polymer Blends, Grafts and Blocks*; Sperling, L. H., Ed.; Plenum Press: New York, 1974; p 281.
(3) Dunn, D. J.; Krause, S. *J. Polym. Sci., Polym. Lett. Ed.* **1974**, *12*, 591.
(4) Krause, S.; Dunn, D. J.; Seyed-Mozzaffari, A.; Biwas, A. M. *Macromolecules* **1977**, *10*, 786.
(5) Bares, J. *Macromolecules* **1975**, *8*, 244.
(6) Toporowski, P. M.; Roovers, J. E. L. *J. Polym. Sci., Polym. Chem. Ed.* **1976**, *14*, 2233.
(7) Hansen, D. R.; Shen, M. *Macromolecules* **1975**, *8*, 903.
(8) Phalip, P.; Favier, J. C.; Sigwalt, P. *Polym. Bull.* **1984**, *12*, 331.
(9) Lau, S. F.; Pathak, J.; Wunderlich, B. *Macromolecules* **1982**, *15*, 1278.
(10) Saeki, S.; Cowie, J. M. G.; McEwen, I. J. *Polymer* **1983**, *24*, 60.
(11) Widmaier, J. M.; Mignard, G. *Eur. Polym. J.* **1987**, *23*, 989.
(12) Lin, J. L.; Roe, R. J. *Polymer* **1988**, *29*, 1227.
(13) Stejskal, E. O.; Schaefer, J.; Sefcik, M. D.; McKay, R. A. *Macromolecules* **1981**, *14*, 275.
(14) Schmidt-Rohr, K.; Clauss, J.; Blumich, B.; Spiess, H. W. *Magn. Reson. Chem.* **1990**, *28*, S3.
(15) Havens, J. R.; VanderHart, D. L. *Macromolecules* **1985**, *18*, 1663.
(16) VanderHart, D. L. *Makromol. Chem., Macromol. Symp.* **1990**, *34*, 125.
(17) Schaefer, J.; Sefcik, M. D.; Stejskal, E. O.; McKay, R. A. *Macromolecules* **1981**, *14*, 188.
(18) Kaplan, S. *Polym. Prepr. (Am. Chem. Soc., Div. Polym. Chem.)* **1984**, *25*, 356.
(19) Voelkel, R. *Angew. Chem., Int. Ed. Engl.* **1988**, *27*, 1468.
(20) Lin, T. S.; Ward, T. C. *Polym. Prepr. (Am. Chem. Soc., Div. Polym. Chem.)* **1983**, *24*, 136.
(21) Tekely, P.; Laupretre, F.; Monnerie, L. *Polymer* **1985**, *26*, 1081.
(22) Dickinson, L. C.; Yang, H.; Chu, C. W.; Stein, R. S.; Chien, J. C. W. *Macromolecules* **1987**, *20*, 1757.
(23) Parmer, J. F.; Dickinson, L. C.; Chien, J. C. W.; Porter, R. S. *Macromolecules* **1989**, *22*, 1078.
(24) Li, S.; Dickinson, L. C.; Chien, J. C. M. *J. Appl. Polym. Sci.* **1991**, *43*, 1111.
(25) Kim, J. K.; Han, C. D. *Macromolecules* **1992**, *25*, 271.
(26) Frye, J. S.; Maciel, G. E. *J. Magn. Reson. Chem.* **1982**, *48*, 125.
(27) Fox, T. G. *Bull. Am. Phys. Soc.* **1956**, *1*, 123.
(28) Suzuki, H.; Miyamoto, Y. *Macromolecules* **1990**, *23*, 1877.
(29) Roland, C. M. *Macromolecules* **1987**, *20*, 2557.
(30) Trask, C. A.; Roland, C. M. *Macromolecules* **1989**, *22*, 256.
(31) Miller, J. B.; McGrath, K. J.; Roland, C. M.; Trask, C. A.; Garroway, A. N. *Macromolecules* **1990**, *23*, 4543.

Registry No. (PαMS-*block*-PS) (block copolymer), 108080-90-6.